

Control of the Stereochemical Impact of the Lone Pair in Lead(II) Tris(pyrazolyl)methane Complexes. Improved Preparation of Na{B[3,5-(CF₃)₂C₆H₃]₄}

Daniel L. Reger,* Terri D. Wright, Christine A. Little, Jaydeep J. S. Lamba, and Mark D. Smith

Department of Chemistry and Biochemistry, University of South Carolina, Columbia, South Carolina 29208

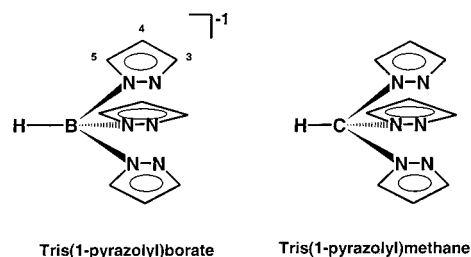
Received January 3, 2001

The reaction of Pb(acac)₂ with 2 equiv of [H(Et₂O)₂]{B[3,5-(CF₃)₂C₆H₃]₄} (HBAr_f) in CH₂Cl₂ followed by addition of 2 equiv of either HC(pz)₃ or HC(3,5-Me₂pz)₃ (pz = pyrazolyl ring) leads to the formation of {Pb[HC(pz)₃]₂}{B[3,5-(CF₃)₂C₆H₃]₄}₂ (**1**) and {Pb[HC(3,5-Me₂pz)₃]₂}{B[3,5-(CF₃)₂C₆H₃]₄}₂ (**2**), respectively. The cation in **1** has a distorted octahedral structure with a stereochemically active lone pair on lead(II). In contrast, the cation in **2** is trigonally distorted octahedral with the lone pair on the lead(II) clearly stereochemically inactive. The driving force for this cation to have a stereochemically inactive lone pair is that in this geometric arrangement the interligand distances between adjacent 3-position methyl groups are close to 4.0 Å, the sum of the van der Waals radii of two methyl groups. To facilitate this chemistry, the synthesis of Na{B[3,5-(CF₃)₂C₆H₃]₄}, needed to prepare HBAr_f, has been dramatically improved. The main change is to add NaBF₄ to the reaction mixture before forming the Grignard from the reaction of magnesium and 3,5-(CF₃)₂C₆H₃Br. The Grignard reacts with the NaBF₄ as it forms, reducing the danger of explosion and leading to a higher isolated yield of the product. Crystallographic information: **1** is triclinic, *P* $\bar{1}$, *a* = 13.0133(6) Å, *b* = 17.2210(7) Å, *c* = 24.7634(11) Å, α = 71.7300(10)°, β = 82.3630(10)°, γ = 70.5120(10)°, *Z* = 2; **2** is triclinic, *P* $\bar{1}$, *a* = 12.756(4) Å, *b* = 13.469(4) Å, *c* = 17.160(5) Å, α = 82.454(7)°, β = 89.904(8)°, γ = 72.995(7)°, *Z* = 1.

Introduction

In 1984 Zuckerman published the structure of Sn(η^5 -C₅Ph₅)₂ in which the two cyclopentadienyl rings were parallel, thus showing that the lone pair on tin(II) was stereochemically inactive, a violation of VSEPR theory.¹ Subsequently, a number of MCp₂ (Cp = substituted cyclopentadienyl ligand) structures with M = Ge, Sn, and Pb have been prepared in which the rings are also parallel.^{2,3} Although in Zuckerman's original paper he argued that the reason for the parallel ring structure was interligand repulsions, more recent work, including theoretical calculations,^{3,4} indicate that this geometry can be observed in complexes with no close contacts between the substituents on the rings. For example, the complex Pb(1,2,4-(Prⁱ)₃C₅H₂)₂ has parallel rings, but there are no interligand methyl group contacts less than 4.17 Å, where the van der Waals radii sum for two methyl groups is 4.0 Å.^{2b} From these results, Hanusa argued against simple steric effects forcing the parallel arrangement and favored crystal packing forces as the dominant factor.^{2b} In an earlier paper, he also compared group 2 and 14 metallocene structures, and argued,^{2a} on the basis of the similarity of the structures of a large number of complexes, that "the confinement of the metal valence electrons of the divalent Group 14 metals

Chart 1



to nondirectional orbitals of high *s*-character" limits their influence on the structures of metallocene complexes.

Understanding the factors that control the stereoactivity of the lone pair in lead(II) chemistry may be important in the design of complexing agents that can remove this toxic metal selectively from biological systems.⁵ We have launched a program aimed at determining whether we can prepare pseudometallocene complexes of the type Pb[tris(pyrazolyl)borate]₂ in which the stereoactivity of the lone pair on lead(II) is controlled by varying the substituents, especially at the 3-position, on tris(pyrazolyl)borate ligands (Tp; Chart 1).⁶

Many groups have compared the donor properties of Cp and Tp ligands, given that they are both formally six electron donor, monoanionic ligands.⁷ Our initial results showed that we could control the impact of the lone pair by changing the pyrazolyl substituents. The complex Pb[HB(pz)₃]₂ (pz = pyrazolyl

(1) Heeg, M. J.; Janiak, C.; Zuckerman, J. J. *J. Am. Chem. Soc.* **1984**, *106*, 4259.

(2) (a) Burkey, D. J.; Hanusa, T. P. *Comments Inorg. Chem.* **1995**, *17*, 41. (b) Burkey, D. J.; Hanusa, T. P.; Huffman, J. C. *Inorg. Chem.* **2000**, *39*, 153 and references therein.

(3) Constantine, S. P.; Cox, H.; Hitchcock, P. B.; Lawless, G. A. *Organometallics* **2000**, *19*, 317 and references therein.

(4) Armstrong, D. R.; Duer, M. J.; Davidson, M. G.; Moncrieff, D.; Russell, C. A.; Stourton, C.; Steiner, A.; Stalke, D.; Wright, D. S. *Organometallics* **1997**, *16*, 3340.

(5) Shimoni-Livny, L.; Glusker, J. P.; Bock, C. W. *Inorg. Chem.* **1998**, *37*, 1853 and reference therein.

(6) (a) Reger, D. L.; Huff, M. F.; Rheingold, A. L.; Haggerty, B. S. *J. Am. Chem. Soc.* **1992**, *114*, 579. (b) Reger, D. L. *Synlett* **1992**, 469.

ring) has a highly distorted 6-coordinate structure. In this structure, there is clearly a gap where the lone pair of electrons is thought to be located and a pattern of long Pb–N bond distances adjacent to the proposed site of the lone pair and short distances opposite this site, the two main characteristics of lead-(II) structures that contain a stereochemically active lone pair.⁶ In contrast, Pb[HB(3,5-Me₂pz)₃]₂ has an octahedral structure in which there is clearly a stereochemically inactive lone pair.⁶ We followed this research with analogous studies using tris-(pyrazolyl)methane ligands (Chart 1), ligands that are isoelectronic to tris(pyrazolyl)borate ligands, but are neutral rather than anionic. Using these ligands, we showed that the cation in {Pb[HC(3,5-Me₂pz)₃]₂}(BF₄)₂ was octahedral, but as observed with the tris(pyrazolyl)borate ligands, the cation in {Pb[HC(pz)₃]₂}(BF₄)₂ has a highly distorted 6-coordinate structure.⁸

Given Hanusa's suggestion that crystal packing is important in determining the solid-state geometries of Group 14 MCp₂ complexes, we found it interesting that both Pb[HB(3,5-Me₂pz)₃]₂ and {Pb[HC(3,5-Me₂pz)₃]₂}(BF₄)₂ crystallize in the highly symmetric R $\bar{3}$ and R $\bar{3}c$ space groups. We decided to prepare complexes of the {Pb[HC(3,5-Me₂pz)₃]₂}²⁺ and {Pb[HC(pz)₃]₂}²⁺ cations with a very different anion other than BF₄⁻ to dramatically change the crystal packing forces. We report here the syntheses and solid-state structures of {Pb[HC(pz)₃]₂}-{B[3,5-(CF₃)₂C₆H₃]₄]₂ (**1**) and {Pb[HC(3,5-Me₂pz)₃]₂}-{B[3,5-(CF₃)₂C₆H₃]₄]₂ (**2**). We also describe a modification of the preparation of Na{B[3,5-(CF₃)₂C₆H₃]₄} that is safer and leads to pure product in very high yield.

Experimental Section

General Procedures. All operations were carried out under a nitrogen atmosphere using either standard Schlenk techniques or a Vacuum Atmospheres HE-493 drybox. All solvents were dried, degassed, and distilled prior to use. Proton chemical shifts are reported in parts per million versus TMS. Lead(II) acetylacetonate (Pb(acac)₂) and 3,5-bis(trifluoromethyl)bromobenzene were purchased from Aldrich Chemicals. HC(pz)₃ and HC(3,5-Me₂pz)₃ were prepared according to our recently reported procedures.⁹ Na{B[3,5-(CF₃)₂C₆H₃]₄} (NaBAr_f) was prepared as outlined below and converted to [H(Et₂O)₂]{B[3,5-(CF₃)₂C₆H₃]₄} (HBAr_f) by the published procedures.¹⁰ Elemental analyses were performed by Robertson Microlit Laboratories, Inc. and Desert Analytics Laboratories. *Warning: The Grignard reagent prepared in situ in the preparation of Na{B[3,5-(CF₃)₂C₆H₃]₄} is potentially explosive.¹¹ Lead(II) compounds are extremely toxic, and care should be used when handling them.*

{Pb[HC(pz)₃]₂}-{B[3,5-(CF₃)₂C₆H₃]₄]₂ (**1**). Pb(acac)₂ (0.10 g, 0.25 mmol) was charged into a round-bottom Schlenk flask and CH₂Cl₂ (10 mL) added. A 2 molar equiv sample of HBAr_f (0.50 g, 0.50 mmol) was placed in a Schlenk flask and dissolved in CH₂Cl₂ (20 mL). This solution was added to the lead suspension and the resulting homogeneous solution allowed to stir for 0.5 h. Hexane (40 mL) was added to this solution, and a white precipitate formed. The mixture was filtered and the white solid dried under reduced pressure. The white solid was redissolved in CH₂Cl₂ (20 mL), and 2 molar equiv of HC(pz)₃ (0.11 g,

0.50 mmol) was added to the solution. This solution was allowed to stir for 24 h at room temperature. The solvent was removed under reduced pressure, and an off-white solid remained (0.40 g, 0.16 mmol, 68%). Crystals suitable for X-ray structural analysis and the analytical sample were grown from a CH₂Cl₂/hexane layered mixture. Mp: 144–149 °C. ¹H NMR (acetone-*d*₆): δ 8.99 (2, s, HC(pz)₃), 8.09, 7.69 (6, 6; d, d; *J* = 2.2, 1.5 Hz; 3,5-H (pz)), 7.79, 7.68 (m, s; 16, 8; 2H, 4H in C₆H₃(CF₃)₂), 6.45 (6, dd, *J* = 2.0, 1.9 Hz; 4-H (pz)). Anal. Calcd for C₈₄H₄₄B₂F₄₈N₁₂Pb: C, 41.97; H, 1.87. Found: C, 42.12; H, 1.14.

{Pb[HC(3,5-Me₂pz)₃]₂}-{B[3,5-(CF₃)₂C₆H₃]₄]₂ (**2**). Pb(acac)₂ (0.10 g, 0.25 mmol) was charged into a round-bottom Schlenk flask, and CH₂Cl₂ (10 mL) was added. A 2 molar equiv sample of HBAr_f (0.50 g, 0.50 mmol) was placed in a Schlenk flask and dissolved in CH₂Cl₂ (20 mL). This solution was added to the lead suspension and the resulting homogeneous solution allowed to stir for 0.5 h. Hexane (40 mL) was added to this solution, and a white precipitate formed. The mixture was filtered and the white solid dried under reduced pressure. The white solid was redissolved in CH₂Cl₂ (20 mL), and 2 molar equiv of HC(3,5-Me₂pz)₃ (0.15 g, 0.50 mmol) was added to the solution. This solution was allowed to stir for 24 h at room temperature. The solvent was removed under reduced pressure, and an off-white solid remained (0.43 g, 0.17 mmol, 69%). Crystals suitable for X-ray structural analysis and the analytical sample were grown from a CH₂Cl₂/hexane layered mixture. Mp: 176–181 °C. ¹H NMR (acetone-*d*₆): δ 8.28 (2, s, HC(3,5-Me₂pz)₃), 7.79, 7.68 (m, s; 16, 8; 2H, 4H in C₆H₃(CF₃)₂), 6.07 (s, 6, 4-H (pz)), 2.80, 2.29 (18, 18; br, s; 3,5-Me (pz)). Anal. Calcd for C₉₆H₆₈B₂F₄₈N₁₂Pb: C, 43.55; H, 2.68. Found: C, 43.65; H, 2.89.

Na{B[3,5-(CF₃)₂C₆H₃]₄}. A 500 mL three-necked flask fitted with a reflux condenser and an addition funnel was charged with Mg (1.01 g, 41.7 mmol), NaBF₄ (0.70 g, 6.4 mmol), and 150 mL of Et₂O. (*Note: All glassware was flame dried prior to use.*) Dibromoethane (0.49 mL, 5.7 mmol) was added, and the flask was heated for several minutes with a heat gun to initiate the reaction. The heat was removed, and 3,5-bis(trifluoromethyl)bromobenzene (6.2 mL, 36 mmol), diluted with 50 mL Et₂O, was added dropwise over ca. 30 min. The addition causes the solution to gently reflux, and once all of the 3,5-bis(trifluoromethyl)-bromobenzene had been added, the reaction mixture was heated with a heating mantle to continue the reflux for an additional 30 min. The heat was then removed and the reaction mixture left to stir overnight at room temperature. The reaction mixture was added to Na₂CO₃ (16 g) in water (200 mL), stirred for 30 min, and filtered. The aqueous layer was extracted with ether (3 × 50 mL), and the combined organic layer was dried over sodium sulfate and treated with decolorizing charcoal. The mixture was filtered and the ether removed under vacuum. The remaining oily-solid was dissolved in 200 mL of benzene, and water was removed with a Stark trap by azeotropic distillation for 2 h. The solvent volume was reduced to 50 mL and the solution cooled to room temperature and filtered via cannula filtration to remove unreacted starting material and other soluble impurities. The remaining white solid was dried under vacuum (5.04 g, 5.6 mmol, 90%). Mp: 300–306 °C. ¹H NMR (acetone *d*₆): δ 7.79 (8, br, 2,6-HB[3,5-(CF₃)₂C₆H₃]₄), 7.67 (4, s, 4-HB[3,5-(CF₃)₂C₆H₃]₄). Anal. Calcd for C₃₂H₁₂F₂₄BNa (sample protected from air): C, 43.37; H, 1.36. Found: C, 43.48; H, 1.61. Anal. Calcd for C₃₂H₁₂F₂₄BNa·2H₂O (sample not protected from air): C, 41.68; H, 1.74. Found: C, 41.43; H, 1.75.

X-ray Structure Determination. Crystal, data collection, and refinement parameters are given in Table 1. A colorless parallelepiped crystal of **1** of dimensions 0.34 mm × 0.10 mm × 0.08 mm and a colorless plate crystal **2** of dimensions 0.32 mm × 0.22 mm × 0.08 mm were epoxied onto the end of a thin glass fiber. The X-ray intensity data were measured at 293 K using a Bruker SMART APEX CCD-based diffractometer system equipped with a Mo target X-ray tube (λ = 0.71073 Å).

The unit cell was initially determined on the basis of reflections harvested from a set of three scans measured in orthogonal wedges of reciprocal space. Subsequently, 2060 data frames for **1** and 1405 data frames for **2** were collected with a scan width of 0.3° in ω and an exposure time of 20 s/frame for **1** and 10 s/frame for **2**. The first 50 frames were recollected at the end of the data set to monitor crystal decay. The raw data frames were integrated with the Bruker SAINT

- (7) (a) Trofimenko, S. *Scorpionates - The Coordination Chemistry of Poly(pyrazolyl)borate Ligands*; Imperial College Press: London, 1999; p 31. (b) Tellers, D. M.; Skoog, S. J.; Bergman, R. G.; Gunnoe, T. B.; Harman, W. D. *Organometallics* **2000**, *19*, 2428.
- (8) Reger, D. L.; Collins, J. E.; Rheingold, A. L.; Liable-Sands, L. M.; Yap, G. P. A. *Inorg. Chem.* **1997**, *36*, 345.
- (9) Reger, D. L.; Grattan, T. C.; Brown, K. J.; Little, C. A.; Lamba, J. J. S.; Rheingold, A. L.; Sommer, R. D. *J. Organomet. Chem.* **2000**, *607*, 120.
- (10) (a) Brookhart, M.; Grant, B.; Vople, J. A. F. *Organometallics* **1992**, *11*, 3920. (b) Hughes, R. P.; Lindner, D. C.; Rheingold, A. L.; Yap, G. P. A. *Inorg. Chem.* **1997**, *36*, 1726.
- (11) Moore, E. J.; Waymouth, R. *Chem. Eng. News* **1997**, *March 17*, 6.

Table 1. Crystallographic Data for the Structural Analyses of $\{\text{Pb}[\text{HC}(\text{pz})_3]_2\}\{\text{B}[3,5-(\text{CF}_3)_2\text{C}_6\text{H}_3]_4\}_2 \cdot 0.7\text{CH}_2\text{Cl}_2$ (**1**) and $\{\text{Pb}[\text{HC}(3,5\text{-Me}_2\text{pz})_3]_2\}\{\text{B}[3,5-(\text{CF}_3)_2\text{C}_6\text{H}_3]_4\}_2 \cdot 2\text{CH}_2\text{Cl}_2$ (**2**)

	1	2
empirical formula	$\text{C}_{84.70}\text{H}_{45.40}\text{B}_2\text{Cl}_{1.40}\text{F}_{48}\text{N}_{12}\text{Pb}$	$\text{C}_{98}\text{H}_{72}\text{B}_2\text{Cl}_4\text{F}_{48}\text{N}_{12}\text{Pb}$
fw	2421.57	2700.29
space group	<i>P</i> 1	<i>P</i> 1
cryst syst	triclinic	triclinic
<i>a</i> , Å	13.0133(6)	12.756(4)
<i>b</i> , Å	17.2210(7)	13.469(4)
<i>c</i> , Å	24.7634(11)	17.160(5)
α , deg	71.7300(10)	82.454(7)
β , deg	82.3630(10)	89.904(8)
γ , deg	70.5120(10)	72.995(7)
<i>V</i> , Å ³	4965.4(4)	2792.7(15)
<i>Z</i>	2	1
cryst color	colorless	colorless
ρ (calcd), g cm ⁻³	1.620	1.606
μ (Mo K α), mm ⁻¹	1.876	1.737
<i>R</i> 1(<i>F</i>), ^a <i>wR</i> 2(<i>F</i> ²) ^a	0.0611, 0.1631	0.0661, 0.1495

^a $R1 = \sum ||F_o| - |F_c|| / \sum |F_o|$, $wR2 = \{ \sum [w(F_o^2 - F_c^2)^2] / \sum [w(F_o^2)^2] \}^{1/2}$; $w = 1 / [\sigma^2(F_o^2) + (aP)^2 + bP]$, where *P* is $[2F_c^2 + \max(F_o^2, 0)]/3$.

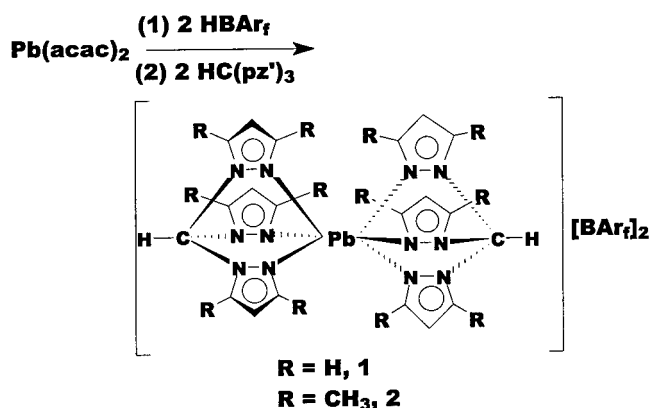
software package (SAINT+ Version 6.02a, Bruker Analytical X-ray Systems, Inc., Madison, WI, 1998) using a narrow-frame integration algorithm, yielding for **1** a total of 51219 reflections to a maximum 2θ angle of 52.9° (0.80 Å resolution), of which 20274 were independent (completeness 99.2%, $R_{\text{int}} = 0.0317$) and 13186 were greater than $2\sigma(I)$. For **2**, a total of 23838 reflections were measured to a maximum 2θ angle of 50.0° (0.84 Å resolution), of which 9802 were independent (completeness 98.0%, $R_{\text{int}} = 0.0880$) and 4828 were greater than $2\sigma(I)$. Corrections for Lorentz and polarization effects were also applied by SAINT. The final triclinic cell constants are based upon the refinement of the XYZ centroids of 5950 reflections for **1** and 2010 reflections for **2** above $10\sigma(I)$. Analysis of the data showed negligible crystal decay during data collection for **1**. Comparison of identical reflections measured at the beginning and at the end of the data collection for **2** showed an average loss of intensity of 5.7%; therefore, a time decay correction was applied. An empirical absorption correction based on the multiple measurement of equivalent reflections was applied to both structures with the program SADABS.

For both structures, the space group *P*1 was assumed and confirmed by successful solution and refinement of the structure. The structures were solved by a combination of direct methods and difference Fourier syntheses, and refined by full-matrix least-squares against F^2 . For **1**, significant disorder of some of the CF₃ groups of the anion was observed; these were modeled as two half-occupied CF₃ groups rotated by 60° relative to one another. A disordered methylene chloride molecule is present which refined to an occupancy of ca. 70%; C–Cl distance restraints were applied to this molecule. For **2**, significant rotational disorder of some of the CF₃ groups of the anion was observed; these were modeled as two partially occupied CF₃ groups rotated by 60° relative to one another. All non-hydrogen atoms were refined with anisotropic displacement parameters; hydrogen atoms were refined using a riding model. All software and sources of the scattering factors are contained in the SHELXTL (5.10) program library (G. Sheldrick, Bruker AXS, Madison, WI).

Results and Discussion

The reaction of $\text{Pb}(\text{acac})_2$ with 2 equiv of $[\text{H}(\text{Et}_2\text{O})_2]\{\text{B}[3,5-(\text{CF}_3)_2\text{C}_6\text{H}_3]_4\}$ (HBAr_f) in CH_2Cl_2 followed by addition of 2 equiv of either $\text{HC}(\text{pz})_3$ or $\text{HC}(3,5\text{-Me}_2\text{pz})_3$ leads to the formation of the desired two complexes $\{\text{Pb}[\text{HC}(\text{pz})_3]_2\}\{\text{B}[3,5-(\text{CF}_3)_2\text{C}_6\text{H}_3]_4\}_2$ (**1**) and $\{\text{Pb}[\text{HC}(3,5\text{-Me}_2\text{pz})_3]_2\}\{\text{B}[3,5-(\text{CF}_3)_2\text{C}_6\text{H}_3]_4\}_2$ (**2**), respectively. These compounds are air-stable, high-melting solids that are soluble in THF, acetone, and CH_2Cl_2 .

As part of our synthetic studies, we have modified the literature preparation¹⁰ of $\text{Na}\{\text{B}[3,5-(\text{CF}_3)_2\text{C}_6\text{H}_3]_4\}$ (NaBAr_f) to



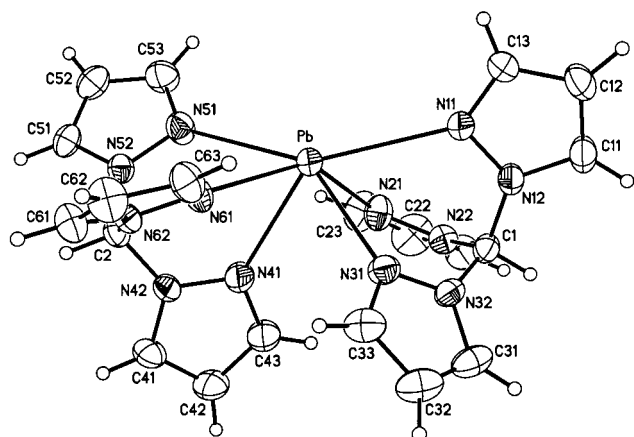
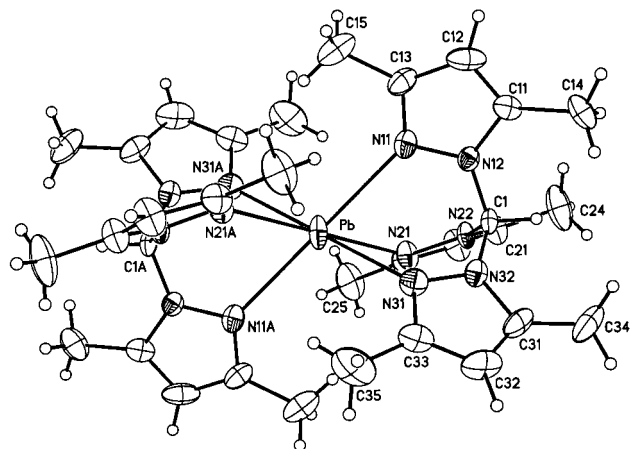
avoid heating large amounts of the potentially explosive Grignard reagent prepared from 3,5-(CF₃)₂C₆H₃Br.¹¹ Specifically, at the start of the reaction NaBF₄ is added to the reaction flask along with ether and the magnesium turnings. The magnesium turnings are activated with C₂H₄Br₂ to ensure that the Grignard reaction initiates immediately upon dropwise addition of 3,5-(CF₃)₂C₆H₃Br to the ether mixture. Presumably, most of the potentially explosive Grignard reagent formed during this addition reacts with the NaBF₄ and does not build up in solution. Residual water and diethyl ether, introduced in the initial workup, are removed by a brief benzene azeotrope procedure.^{10b} The benzene is removed by filtration, yielding an off-white solid in 90% yield that is pure by NMR and elemental analysis (the literature yield is 70% obtained on a solid not purified as indicated above¹⁰). Monitoring each stage of the workup by NMR shows that prior to the benzene filtration step impurities containing the 3,5-(CF₃)₂C₆H₃ group are present, impurities that are removed by this procedure. Thus, our new reaction conditions not only increase the safety of the procedure, but improve the yield of pure product. Three other important points were determined in our efforts to improve this preparation: (1) The excess of 3,5-(CF₃)₂C₆H₃Br (25.6 mmol required based on NaBF₄, 36 mmol used) reported in the literature preparation¹⁰ appears to be necessary to obtain the high yields reported here. (2) The Na{B[3,5-(CF₃)₂C₆H₃]₄} solid that has been dried by the benzene azeotrope procedure is much less soluble in CH₂Cl₂ than the solid taken into this procedure. (3) We have shown by elemental analysis that pure Na{B[3,5-(CF₃)₂C₆H₃]₄} as prepared here picks up 2 equiv of water when handled in air.

Structure of $\{\text{Pb}[\text{HC}(\text{pz})_3]_2\}\{\text{B}[3,5-(\text{CF}_3)_2\text{C}_6\text{H}_3]_4\}_2$ (1**).** Figure 1 shows the ORTEP diagram of the cation in $\{\text{Pb}[\text{HC}(\text{pz})_3]_2\}\{\text{B}[3,5-(\text{CF}_3)_2\text{C}_6\text{H}_3]_4\}_2$ (**1**), and selected bond distances and angles are shown in Table 2. The lead(II) is 6-coordinate with a highly asymmetric arrangement of the nitrogen donor atoms. As is typical of distorted lead(II) structures, the three Pb–N bond distances adjacent to the “open space” in the structure are longer (average 2.70 Å) than those away from it (average 2.53 Å). The intraligand bond angles are fairly similar, ranging from 68.23(16)° to 72.71(17)° (average 69.8°); however, the interligand bond angles vary from 74.25(18)° to 146.60(16)°.

The structure of **1** is fairly similar to that of $\{\text{Pb}[\text{HC}(\text{pz})_3]_2\}\{\text{BF}_4\}_2$ (**3**; Table 2),^{6a} although the structure of **3** is centrosymmetric. The average Pb–N bond distance in **1** is 2.62 Å with a range of values from 2.499(5) to 2.790(5) Å, and for **3** the average is 2.69 Å with a much smaller range of 2.609(5)–2.789(5) Å. The average intraligand bond angle for **1** (69.8°) is 2.1° greater than for **3** (67.7°). The biggest difference between the two structures is in the range of the interligand bond angles,

Table 2. Selected Bond Distances and Bond Angles for {Pb[HC(pz)₃]₂}{B[3,5-(CF₃)₂C₆H₃]₂} (**1**) and {Pb[HC(pz)₃]₂}(BF₄)₂ (**3**)

	1	3		1	3
			Bond Distances (Å)		
Pb–N(11)	2.499(5)	2.789(5)	Pb–N(51)	2.586(5)	
Pb–N(21)	2.790(5)	2.660(5)	Pb–N(61)	2.619(5)	
Pb–N(31)	2.514(5)	2.609(5)	intraligand donor N···N av distance	3.00	3.00
Pb–N(41)	2.692(5)		Pb distance out of N ₃ donor plane	1.96	2.05
			Selected Bond Angles (deg)		
N(11)–Pb–N(21)	68.81(16)	67.8(2)	N(11)–Pb–N(61,21A)	134.95(16)	119.0(2)
N(11)–Pb–N(31)	72.71(17)	65.5(2)	N(21)–Pb–N(41,31A)	74.43(19)	78.7(2)
N(21)–Pb–N(31)	68.23(16)	69.8(2)	N(21)–Pb–N(51,11A)	104.93(17)	119.0(2)
N(41)–Pb–N(51)	69.14(17)		N(21)–Pb–N(61,21A)	142.73(19)	140.9(2)
N(41)–Pb–N(61)	70.50(15)		N(31)–Pb–N(41,31A)	74.25(18)	72.0(2)
N(51)–Pb–N(61)	69.39(17)		N(31)–Pb–N(51,11A)	142.56(17)	132.5(2)
N(11)–Pb–N(41,31A)	133.36(16)	132.5(2)	N(31)–Pb–N(61,21A)	88.86(17)	78.7(2)
N(11)–Pb–N(51,11A)	146.60(16)	161.4(2)	av Fe–N(1)–N(2)–C(1) torsion	174	167

**Figure 1.** ORTEP diagram of {Pb[HC(pz)₃]₂}²⁺ with thermal ellipsoids drawn at the 30% probability level.**Figure 2.** ORTEP diagram of {Pb[HC(3,5-Me₂pz)₃]₂}²⁺ with thermal ellipsoids drawn at the 30% probability level.

which at 74.25(18)–146.60(16)° for **1** is much lower than that for **3**, 72.0(2)–161.4(2)°. Clearly, crystal lattice forces in these compounds impact the structures of the cations, but both have highly distorted arrangements about the lead(II).

Structure of {Pb[HC(3,5-Me₂pz)₃]₂}{B[3,5-(CF₃)₂C₆H₃]₂} (2**).** Figure 2 shows the ORTEP diagram of the cation in {Pb[HC(3,5-Me₂pz)₃]₂}{B[3,5-(CF₃)₂C₆H₃]₂} (**2**), and selected bond distances and angles are shown in Table 3. The lead(II) is 6-coordinate with a highly symmetric pseudooctahedral arrangement of the nitrogen donor atoms. The three Pb–N distances are nearly equal. The chelate rings restrict the intraligand N–Pb–N bond angles to an average of 72.1° with cis interligand N–Pb–N bond angles averaging 107.9°. All trans

N–Pb–N angles are 180°, as required by the symmetry, making the structure a trigonally distorted octahedron. *The lone pair on the lead(II) is clearly stereochemically inactive.*

Although **2** is not in the highly symmetric $R\bar{3}c$ space group as is {Pb[HC(3,5-Me₂pz)₃]₂}(BF₄)₂ (**4**),^{6a} the bond distances and angles about the lead(II) center in the two structures are generally similar. The average Pb–N distance in **2** of 2.59 Å is 0.05 Å shorter than that found in **4**. The range of values in the lower symmetry **2** is only 0.02 Å. The cis interligand N–Pb–N bond angles in **2** have a range of 2.4° and average 72.1°, just 0.3° less than in **4**.

There is a surprisingly large difference in the two structures in the degree of tilting the pyrazolyl rings make away from an ideal C_{3v} type arrangement. In the absence of tilting, the Pb–N(*n*1)–N(*n*2)–C(*n*1) torsion angles (where *n* denotes the ring number) would be 180°, and the metal atom would reside in the planes defined by the pyrazolyl rings, planes that also contain the lone pair on the donor nitrogen atom. In complex **2** this angle averages 159°, whereas in **4** it is 130°. A consequence of the difference in tilting is that the average N···N intraligand nonbonding distance increases from 3.04 Å in **2** to 3.12 Å in **4**. This increased tilting is likely responsible for the longer Pb–N bond distances in **4**. Another change caused by the tilting is in the nonbonding distances between adjacent interligand 3-methyl groups. For **2** these distances average 4.02 Å, nearly exactly the van der Waals radii of two methyl groups, but decrease to 3.93 Å in **4**.

We have previously commented on the fact that in octahedral {M[HC(3,5-Me₂pz)₃]₂}^{*m*+} and M[HB(3,5-Me₂pz)₃]₂ complexes this ring tilting increases with increasing size of the metal.^{6,8,12,16} Table 4 shows data for cations in complexes of the HC(3,5-Me₂pz)₃ ligand that we have characterized, to date. The bite size of this ligand is largely fixed by the size of the pyrazolyl ring, the C–N bond distances, and the N–C–N bond angles, but is increased by this tilting to accommodate large metal ions. It is clear from these results with **2** and **4** that factors other than metal size are important in determining the degree of tilting. The difference in the tilting and, to a lesser extent, the Pb–N bond distances between **2** and **4** are a surprisingly large consequence of changes in the crystal packing forces. The

- (12) Reger, D. L.; Collins, J. E.; Layland, R.; Adams, R. D. *Inorg. Chem.* **1996**, *35*, 1372.
- (13) Reger, D. L.; Little, C. A.; Rheingold, A. L.; Liable-Sands, L. M.; Smith, M. D. Unpublished results.
- (14) Reger, D. L.; Collins, J. E.; Yap, G. P. A. *Organometallics* **1997**, *16*, 349.
- (15) Reger, D. L.; Collins, J. E.; Myers, S. M.; Rheingold, A. L.; Liable-Sands, L. M. *Inorg. Chem.* **1996**, *35*, 4904.
- (16) Reger, D. L.; Little, C. A.; Young V.; Pink, M. *Inorg. Chem.* **2001**, *40*, 2870.

Table 3. Selected Bond Distances and Bond Angles for {Pb[HC(3,5-Me₂pz)₃]₂}{B[3,5-(CF₃)₂C₆H₃]₄]₂} (**2**) and {Pb[HC(3,5-Me₂pz)₃]₂}(BF₄)₂ (**4**)

	2	4		2	4
Bond Distances (Å)					
Pb–N(11)	2.600(6)	2.635(7)	intraligand donor N···N av distance	3.04	3.12
Pb–N(21)	2.581(6)		Pb distance out of N3 donor plane	1.90	1.93
Pb–N(31)	2.577(7)				
Selected Bond Angles (deg)					
N(11)–Pb–N(21)	73.32(19)	72.4(3)	N(21)–Pb–N(21A)	180.0	
N(11)–Pb–N(31)	70.9(2)		N(21)–Pb–N(31A)	108.00(19)	
N(21)–Pb–N(31)	72.00(19)		N(31)–Pb–N(31A)	180.0	
N(11)–Pb–N(11A)	180.0	180.0	Pb–N(11)–N(12)–C(11) torsion	166.4	130.1
N(11)–Pb–N(21A)	106.68(19)	107.6(3)	Pb–N(21)–N(22)–C(21) torsion	156.0	
N(11)–Pb–N(31A)	109.1(2)		Pb–N(31)–N(32)–C(31) torsion	155.2	

Table 4. Average M–N–N–C Torsion Angles (deg), Average M–N Bond Distances (Å), and Average Intraligand N···N Distances (Å) of Selected {M[HC(3,5-Me₂pz)₃]₂}^{m+} Complexes

compound	M–N–N–C torsion angle	M–N distance	N···N distance	ref
{Ti[HC(3,5-Me ₂ pz) ₃] ₂ } (PF ₆)	123	2.92	3.24	12
{K[HC(3,5-Me ₂ pz) ₃] ₂ } (PF ₆)	127	2.82	3.21	13
{Pb[HC(3,5-Me ₂ pz) ₃] ₂ } (BF ₄) ₂	130	2.635	3.12	8
{Pb[HC(3,5-Me ₂ pz) ₃] ₂ } (BARf) ₂	159	2.59	3.04	this work
{Ag[HC(3,5-Me ₂ pz) ₃] ₂ } (O ₃ SCF ₃)	137	2.51	3.12	14
{Na[HC(3,5-Me ₂ pz) ₃] ₂ } (I)	149	2.49	3.10	13
{Cd[HC(3,5-Me ₂ pz) ₃] ₂ } (BF ₄) ₂	141	2.32	2.98	15
{Fe[HC(3,5-Me ₂ pz) ₃] ₂ } (BF ₄) ₂ (high spin)	169	2.18	2.91	16
{Fe[HC(3,5-Me ₂ pz) ₃] ₂ } (BF ₄) ₂ (low spin)	178	1.98	2.72	16

Table 5. Average Pb–N Distances (Å)

{Pb[HC(pz) ₃] ₂ }{B[3,5-(CF ₃) ₂ C ₆ H ₃] ₄] ₂ } (1)	2.62
{Pb[HC(pz) ₃] ₂ }(BF ₄) ₂ (3)	2.69
Pb[HB(pz) ₃] ₂ (5)	2.61
{Pb[HC(3,5-Me ₂ pz) ₃] ₂ }{B[3,5-(CF ₃) ₂ C ₆ H ₃] ₄] ₂ } (2)	2.59
{Pb[HC(3,5-Me ₂ pz) ₃] ₂ }(BF ₄) ₂ (4)	2.635(7) ^a
Pb[HB(3,5-Me ₂ pz) ₃] ₂ (6)	2.610(5) ^a

^a Exact distance given as all Pb–N distances are equivalent.

potential energy surface for these changes must be quite soft, with these large changes in tilting and modest change in bond distances not impacting importantly on the stability of the coordination complex. A recent paper has drawn a somewhat similar conclusion in a study of samarium complexes of the [HB(3,5-Me₂pz)₃][−] ligand.¹⁷

Table 5 compares the average Pb–N distances in the six structures discussed here. Given that the lone pair is in an orbital containing some 6p character in distorted lead(II) structures, it is expected that the Pb–N bond distances will be *shorter* in these structures (more s character, an orbital with a lesser radial extension, in the bonds) compared to symmetrical structures in which the lone pair is in a pure 6s orbital.^{5,18} In addition, the methyl-substituted complexes, the complexes that are symmetrical, have greater interligand repulsions from the 3-position methyl groups, possibly also leading to longer Pb–N bonds. There is no indication from the data in Table 5 that either factor causes the Pb–N bonds to be longer in the symmetrical structures. These results support calculations that indicate that in distorted structures the amount of mixing of the p orbital into the lone pair orbital is small.⁵

(17) Hillier, A. C.; Liu, S.-Y.; Sella, A.; Elsegood, M. R. *J. Inorg. Chem.* **2000**, *39*, 2635.

(18) Hancock, R. D.; Shaikjee, M. S.; Dobson, S. M.; Boeyens, J. C. A. *Inorg. Chim. Acta* **1988**, *154*, 229.

Conclusion

Drastically changing the characteristics of the counterion from [BF₄][−] to {B[3,5-(CF₃)₂C₆H₃]₄][−], thus dramatically changing the crystal lattice forces, changes the details of the structures of the two lead(II) cations, but the change does not impact whether the lone pair is stereochemically active or not. Most importantly, {Pb[HC(3,5-Me₂pz)₃]₂}²⁺ has a trigonally distorted octahedral structure in both cases. The change from a distorted structure in unsubstituted **1** and **3** to a structure with a clearly stereochemically inactive lone pair in **2** and **4** is *dominated by forces within the cations*. Specifically, in the octahedral structures adopted by **2** and **4** the interligand distances between adjacent 3-position methyl groups are close to 4.0 Å, the sum of the van der Waals radii of two methyl groups. It appears that the driving forces for these 6-coordinate complexes to have a stereochemically inactive lone pair in **2** and **4** are these interligand interactions within each cation and not crystal packing forces. A similar conclusion was also made in a recent survey of structures of known lead(II) coordination complexes,⁵ a conclusion now verified by our two additional structures. In the absence of these forces in **1** and **3** the lone pair becomes stereochemically active, producing the distorted structure generally found for PbN₆ central cores with chelating ligands lacking bulky substituents.⁵

Acknowledgment. We thank the National Science Foundation (Grant CHE-9727325) for support. The Bruker CCD single-crystal diffractometer was purchased using funds provided by the NSF Instrumentation for Materials Research Program through Grant DMR:9975623.

Supporting Information Available: Two X-ray crystallographic files in CIF format. This material is available free of charge via the Internet at <http://pubs.acs.org>.

IC0100121